Supporting information

Design and fabrication of MoO_4^{2-}-intercalated LDHs nanosheets coated on Co_9S_8 nanotubes with enhanced cycle stability for high performance supercapacitors

Lei Wu [a], Linli Chen [a], Hao Chen [a], Guochang Li [a], Wenna Zhao [b,*], Lei Han [a,*]

[a] School of Materials Science & Chemical Engineering, Ningbo University, Ningbo, Zhejiang 315211, China

[b] School of Biological and Chemical Engineering, Ningbotech University, Ningbo, Zhejiang 315100, China

* Corresponding Author. E-mail: wnzhao@nit.zju.edu.cn; hanlei@nbu.edu.cn

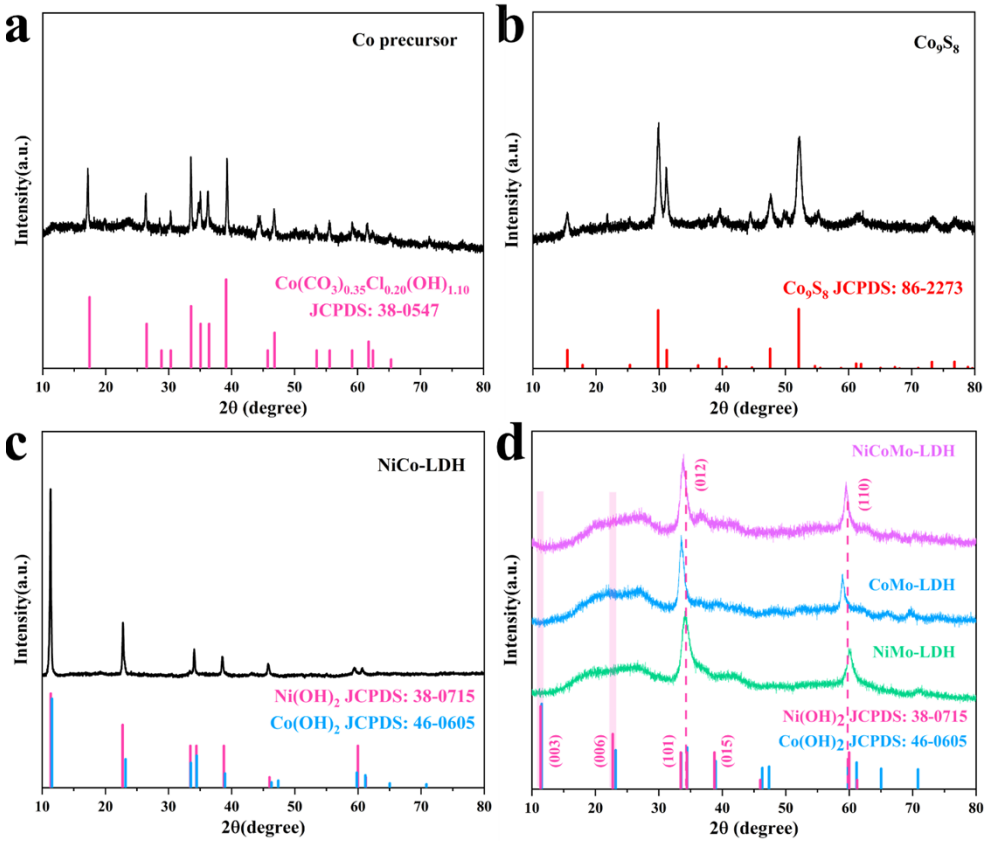

Fig. S1 XRD images of Co precursor, Co_9S_8, NiCo-LDH and MoO_4^{2-}-intercalated LDHs.

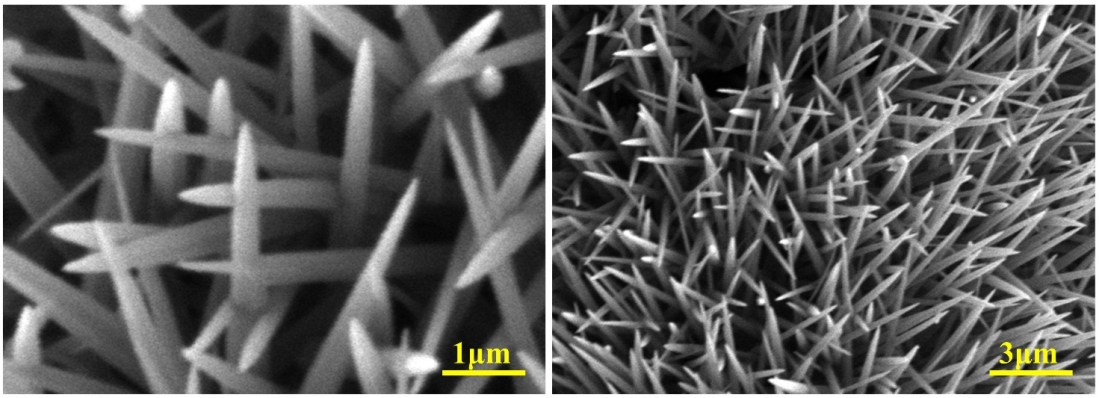

Fig. S2 SEM images of the Co precursor.

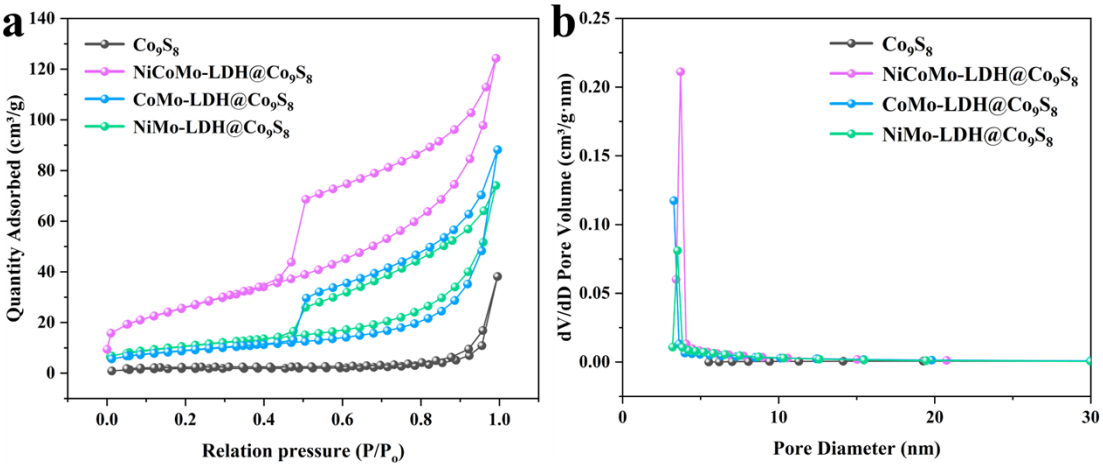

Fig. S3 (a) Nitrogen adsorption-desorption isotherms of Co_9S_8 and MoO_4^{2-}-intercalated LDHs@Co_9S_8; (b) Pore diameter distribution of Co_9S_8 and MoO_4^{2-}-intercalated LDHs@Co_9S_8.

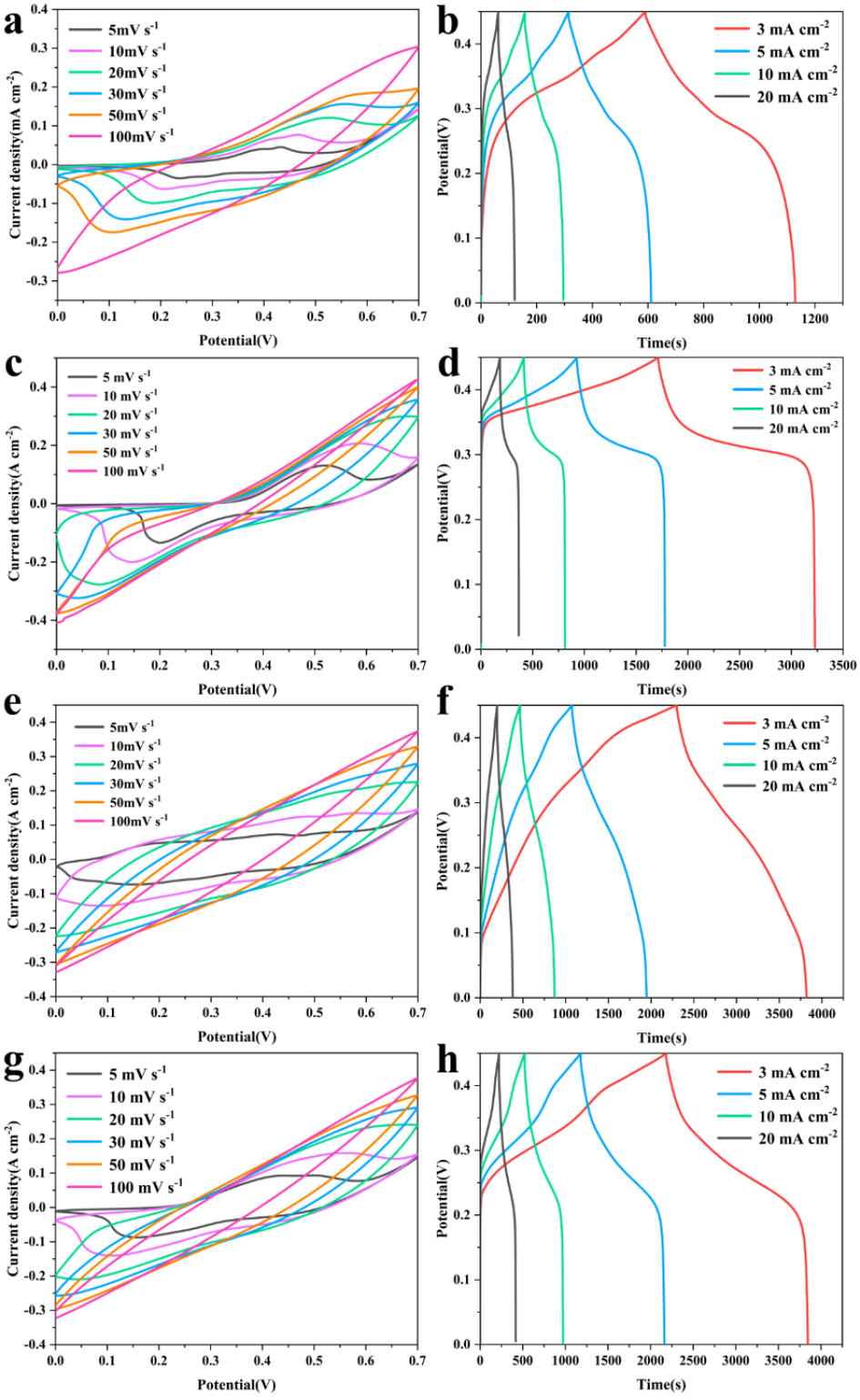

Fig. S4 (a) CV and (b) GCD curves of Co_9S_8, (c) CV and (d) GCD curves of NiMo-LDH@Co_9S_8, (e) CV and (f) GCD curves of CoMo-LDH@Co_9S_8, (g) CV and (h) GCD curves of NiCoMo-LDH@Co_9S_8.

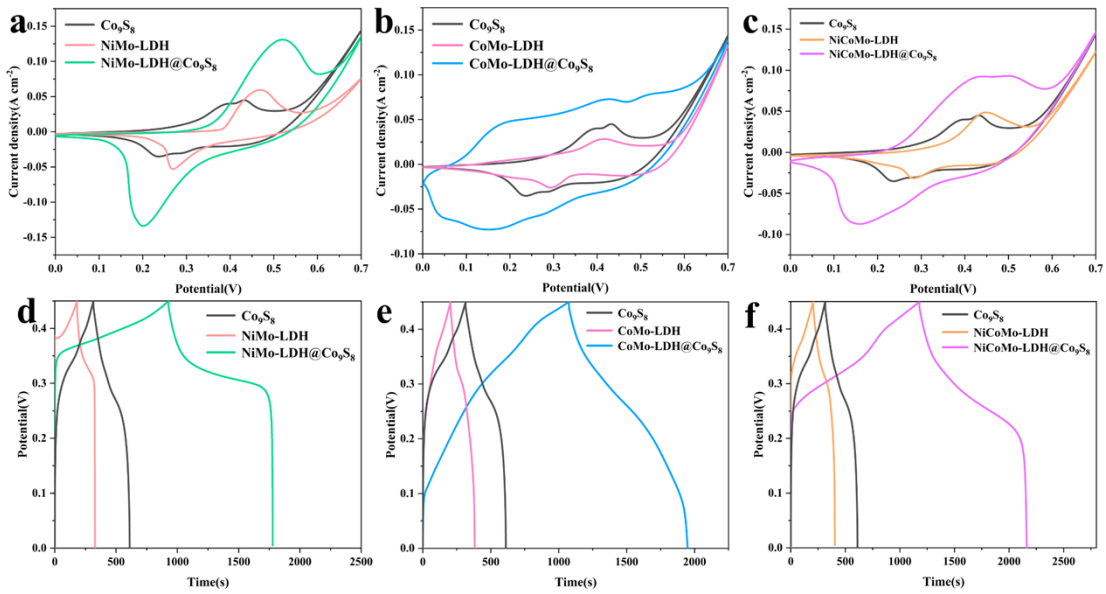

Fig. S5 (a, b, c) CV curves comparing of Co_9S_8, LDH and LDH@Co_9S_8 at 5 mV s^{-1}; (b, d, f) GCD curves comparing of Co_9S_8, LDH and LDH@Co_9S_8 at 5mA cm^{-2}.

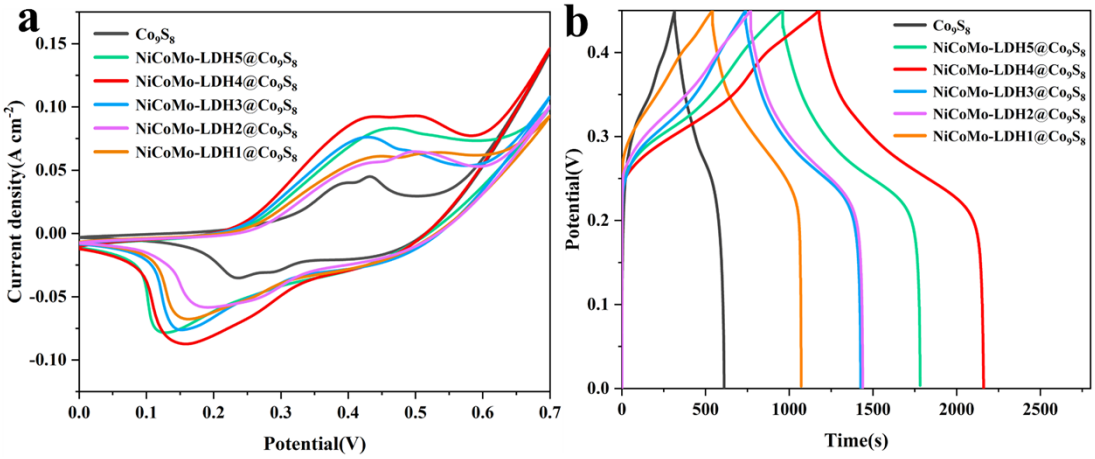

Fig. S6 (a) CV curves of NiCoMo-LDH@Co_9S_8 with different contents of MoO_4^{2-} at 5mV s^{-1}; (b) GCD curves of NiCoMo-LDH@Co_9S_8 with different contents of MoO_4^{2-} at 5mA cm^{-2}.

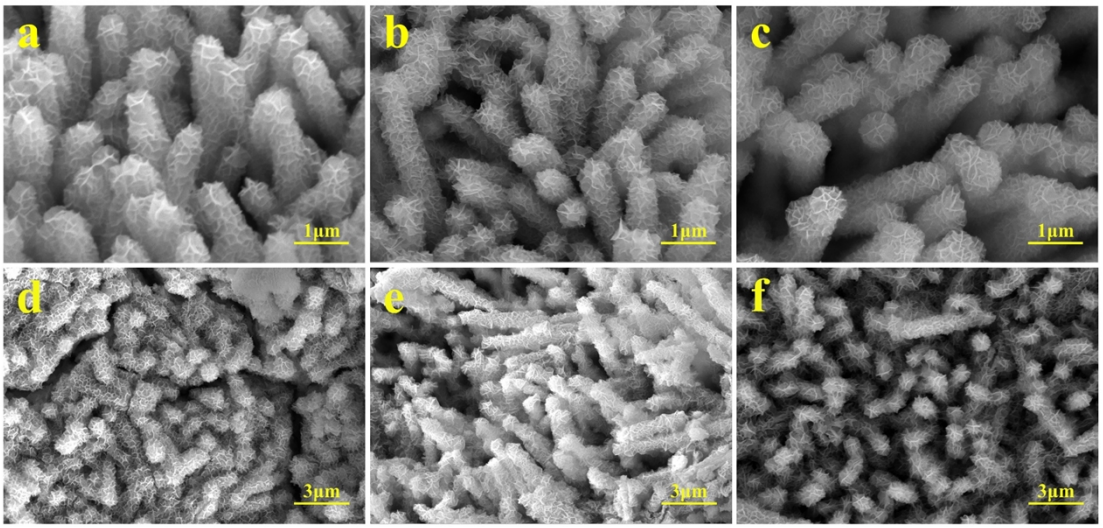

Fig. S7 SEM images of (a) NiMo-LDH@Co_9S_8, (b) CoMo-LDH@Co_9S_8 and (c) NiCoMo-LDH@Co_9S_8 before 5000 cycles; SEM images of (d) NiMo-LDH@Co_9S_8, (e) CoMo-LDH@Co_9S_8 and (f) NiCoMo-LDH@Co_9S_8 after 5000 cycles, respectively.

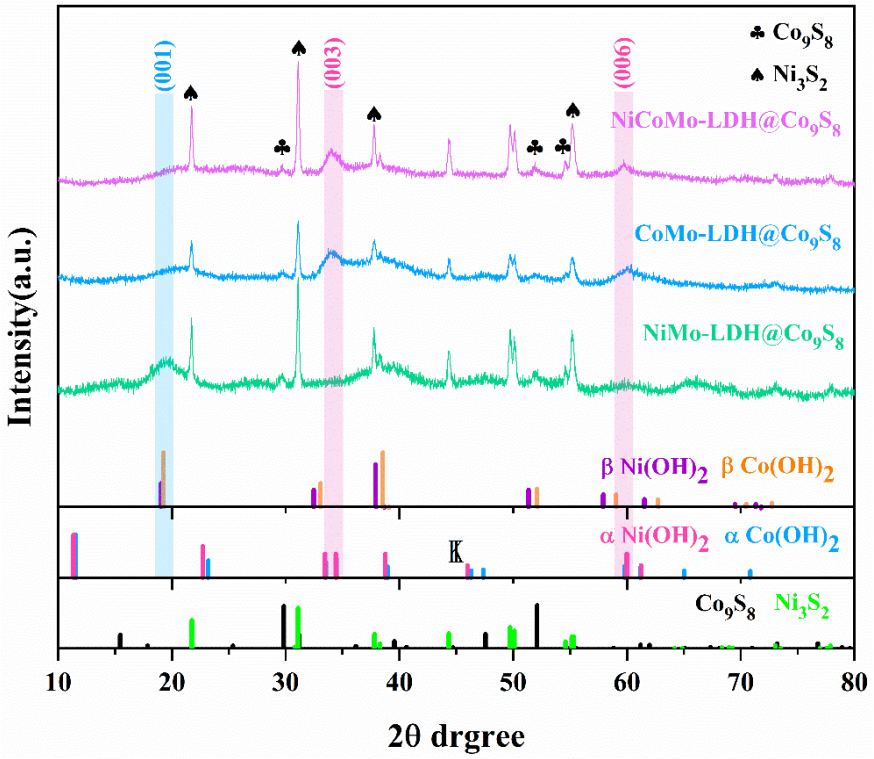

Fig. S8 XRD of MoO_4^{2-}-intercalated LDHs@Co_9S_8 after 5000 cycles.

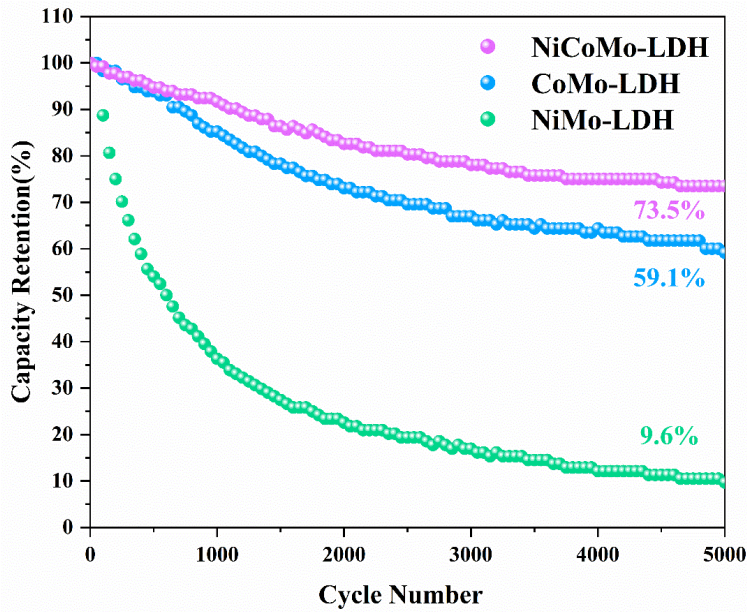

Fig. S9 The cycle stability of NiMo-LDH, CoMo-LDH and NiCoMo-LDH as electrode materials.

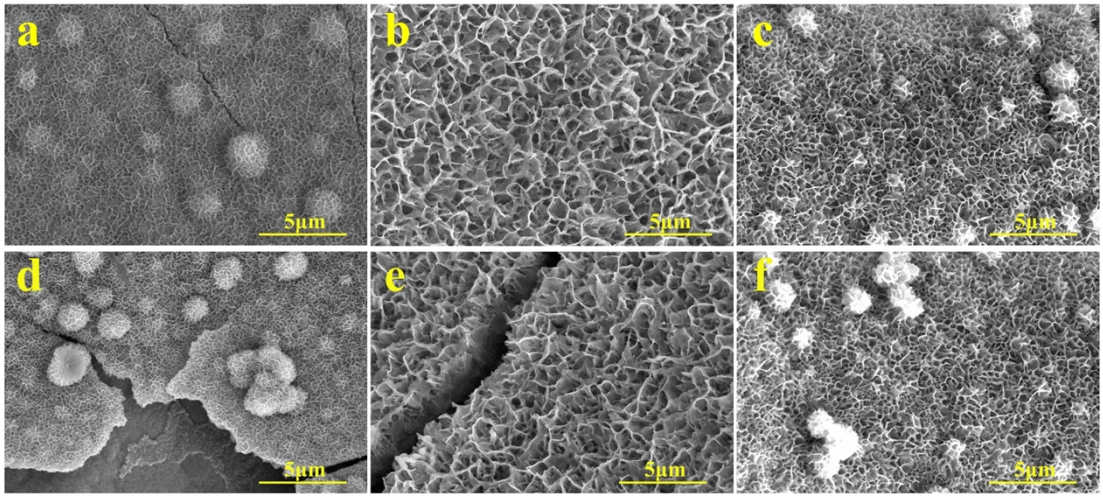

Fig. S10 SEM images of (a) NiMo-LDH, (b) CoMo-LDH and (c) NiCoMo-LDH before 5000 cycles; SEM images of (d) NiMo-LDH, (e) CoMo-LDH and (f) NiCoMo-LDH after 5000 cycles, respectively.

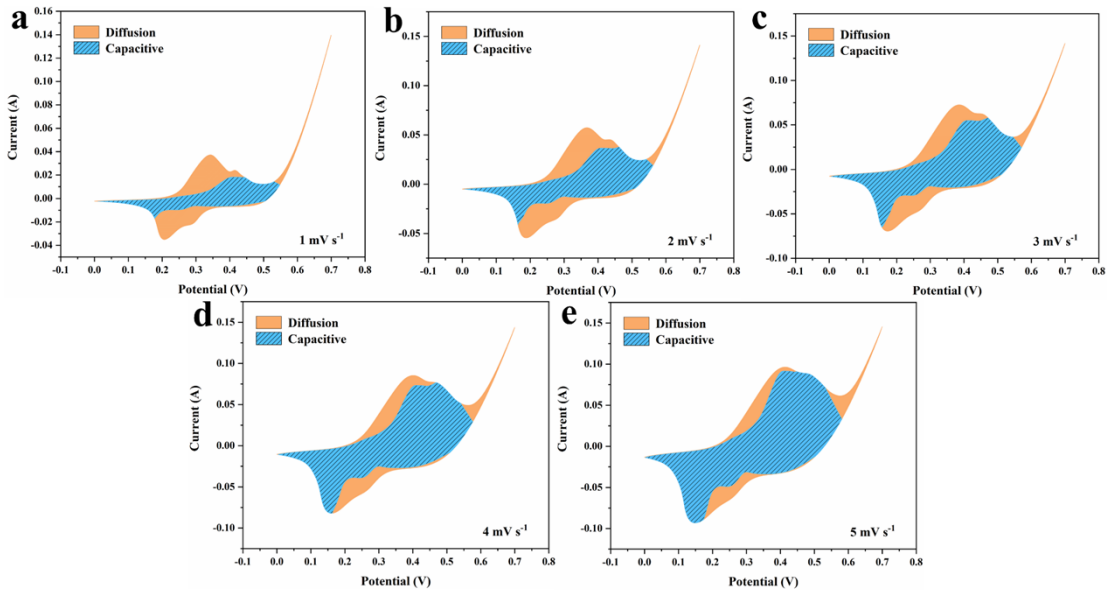

Fig. S11 Capacitive contribution (bule) during charge storage at (a) 1 mV s^{-1}, (b) 2 mV s^{-1}, (c) 3 mV s^{-1}, (d) 4 mV s^{-1}, (e) 5 mV.

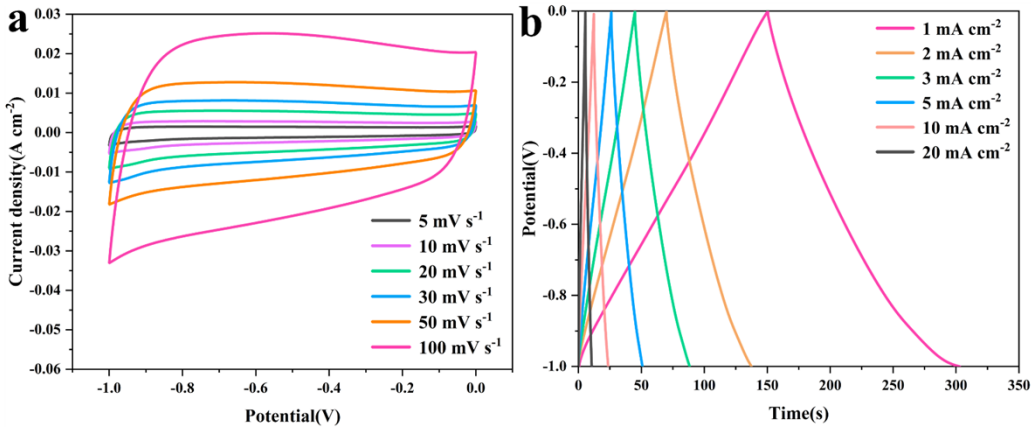

Fig. S12 Electrochemical performance of AC: (a) CV curves; (b) GCD curves.

Table S1 The atomic ratio of Co, Ni, Mo, O and S in NiCoMo-LDH@Co_9S_8, CoMo-LDH@Co_9S_8, NiMo-LDH@Co_9S_8 obtained by XPS test.

Element	NiCoMo-LDH@Co_9S_8	CoMo-LDH@Co_9S_8	NiMo-LDH@Co_9S_8
Co	10.42%	24.99%	4.32%
Ni	13.89%	5.47%	19.34%
Mo	5.44%	6.21%	3.84%
O	64.95%	66.94%	68.91%
S	5.28%	4.92%	3.56%

Table S2 Comparison of different electrode materials related to NiCoMo-LDH@Co_9S_8.

Electrode materials	Capacitance (F cm^{-2})	Current density (mA cm^{-2})	Cyclic stability	Ref
CoO@NiCo LDH	9.42 F cm^{-2}	3 mA cm^{-2}	88.76% (5000 cycles)	[1]
NC LDH NSs@Ag@CC	10.95 F cm^{-2}	3 mA cm^{-2}	80.47% (2000 cycles)	[2]
Co_9S_8@MnO_2	0.80 F cm^{-2}	2 mA cm^{-2}	91.4% (5000 cycles)	[3]
NiMn-LDH@CuO/CF	6.07 F cm^{-2}	2 mA cm^{-2}	89.22% (8000 cycles)	[4]
Ni_3S_2/CoFe LDH/NF	5.08 F cm^{-2}	2 mA cm^{-2}	89.8% (8000 cycles)	[5]
Ag@NCM-LDH MFs@NSs/NF	6.40 F cm^{-2}	5 mA cm^{-2}	88.8% (15000 cycles)	[6]
NiV LDHs@P-NF	2.85 F cm^{-2}	20 mA cm^{-2}	Rarely decrease (5000 cycles)	[7]
Co_9S_8/NF	7.36 F cm^{-2}	2 mA cm^{-2}	/	[8]
CC/NiCoP@NiCo-LDH	4.68 F cm^{-2}	1 mA cm^{-2}	81.1% (5000 cycles)	[9]
NiCoMo-LDH@Co_9S_8//AC	11.0 F cm^{-2}	3 mA cm^{-2}	94.4% (5000 cycles)	This work

References

[S1] Jiao, Z.; Chen, Y.; Du, M.; Demir, M.; Yan, F.; Xia, W.; Zhang, Y.; Wang, C.; Gu, M.; Zhang, X.; Zou, J. 3D hollow NiCo LDH nanocages anchored on 3D CoO sea urchin-like microspheres: A novel 3D/3D structure for hybrid supercapacitor electrodes. *J. Colloid Interface Sci.* **2023**, *633*, 723-736.

[S2] Sekhar, S. C.; Nagaraju, G.; Yu, J. S. Conductive silver nanowires-fenced carbon cloth fibers-supported layered double hydroxide nanosheets as a flexible and binder-free electrode for high-performance asymmetric supercapacitors. *Nano Energy* **2017**, *36*, 58-67.

[S3] Li, Q.; Liu, M.; Huang, F.; Zuo, X.; Wei, X.; Li, S.; Zhang, H. Co_9S_8@MnO_2 core-shell defective heterostructure for High-Voltage flexible supercapacitor and Zn-ion hybrid supercapacitor. *Chem. Eng. J.* **2022**, *437*, 135494.

[S4] Zhang, A.; Zheng, W.; Yuan, Z.; Tian, J.; Yue, L.; Zheng, R.; Wei, D.; Liu, J. Hierarchical NiMn-layered double hydroxides@CuO core-shell heterostructure in-situ generated on $Cu(OH)_2$ nanorod arrays for high performance supercapacitors. *Chem. Eng. J.* **2020**, *380*, 122486.

[S5] Wang, Y.; Zhang, W.; Guo, X.; Liu, Y.; Zheng, Y.; Zhang, M.; Li, R.; Peng, Z.; Zhao, Y. Construction of high-performance asymmetric supercapacitor based on the hierarchical Ni_3S_2/CoFe LDH/Ni foam hybrid. *Appl. Surf. Sci.* **2021**, *561*, 150049.

[S6] Ramulu, B.; Sekhar, S. C.; Arbaz, S. J.; Yu, J. S. Nano-Ag laminated ternary layered double hydroxides for hybrid supercapacitors. *Chem. Eng. J.* **2021**, *420*, 130376.

[S7] Wang, G.; Jin, Z.; Guo, Q. Ordered Self-supporting NiV LDHs@P-Nickel foam

Nano-array as High-Performance supercapacitor electrode. *J. Colloid Interface Sci.* **2021**, *583*, 1-12.
[S8] Aloqayli, S.; Ranaweera, C. K.; Wang, Z.; Siam, K.; Kahol, P. K.; Tripathi, P.; Srivastava, O. N.; Gupta, B. K.; Mishra, S. R.; Perez, F.; Shen, X.; Gupta, R. K. Nanostructured cobalt oxide and cobalt sulfide for flexible, high performance and durable supercapacitors. *Energy Storage Mater.* **2017**, *8*, 68-76.
[S9] Gao, X.; Zhao, Y.; Dai, K.; Wang, J.; Zhang, B.; Shen, X. NiCoP nanowire@NiCo-layered double hydroxides nanosheet heterostructure for flexible asymmetric supercapacitors. *Chem. Eng. J.* **2020**, *384*, 123373.